ISSN 0145-8752, Moscow University Geology Bulletin, 2009, Vol. 64, No. 5, pp. 296–305. © Allerton Press, Inc., 2009.
Original Russian Text © V.B. Piip, 2009, published in Vestnik Moskovskogo Universiteta. Geologiya, 2009, No. 5, pp. 26–35.

Structure of the Siberian Upper Mantle from Superlong Seismic Profile Data

V. B. Piip

Department of Seismometry and Geoacoustics, Faculty of Geology, Moscow State University, Moscow, 119991 Russia
e-mail: piip@list.ru

Received February 6, 2009

Abstract—The paper discusses the mantle structure along superlong seismic profiles in Russia examined using the method of homogenous functions. Two-dimensional heterogeneous sections of the upper mantle were calculated from travel-time curves to a depth of 500–600 km with allowance for the Earth's curvature without using any a priory information. The presentation of sections as surfaces with a shaded relief combined with velocity contours allowed discerning the principal interfaces in the lithosphere and in the upper mantle, the internal structure of layers, and local heterogeneities of different shapes (convective cells and slabs) in the sections.

Key words: seismic interpretation, upper mantle, superlong seismic profiles, tectonics.

DOI: 10.3103/S0145875209050044

INTRODUCTION

Seismic waves from nuclear explosions were recorded in the Soviet Union in order to obtain information on the deep structure of the Earth. The length of the recorded first-arrival travel-time curves exceeded 3500 km. Seismic P-waves penetrate into the mantle and cover it to its base. We have to take into account the Earth's curvature when interpreting these data. At the same time, many methods and algorithms are operable only in the planar Earth, including the method of homogeneous functions. Some publications have presented formulas for transformations for inversion from a spherically symmetrical Earth to a planar model and inversely for the purpose of algorithms and methods application to a planar Earth and then transformation of the result to a spherically symmetrical Earth.

This paper shows that these transformations are correct in the case of two-dimensional arbitrary velocity distribution within a semicircle. These transformations were used for inversion of Jeffreys–Bullen travel-time curves by the method of homogeneous functions and for interpreting superlong travel-time curves along five profiles.

Many authors have examined the mantle structure along superlong travel-time curves in Russia [Vinnik and Egorkin, 1980; Egorkin et al., 1984; Mechie et al., 1993; Pavlenkiova et al., 1996]. However, the 2D sections were presented largely to depths of 200–300 km. Deeper mantle layers are characterized, as a rule, by 1D-velocity dependences or are spherically symmetrical. Therefore, the relief of the transitional layer boundary between the upper and lower mantle, as well as the upper mantle structure below the asthenosphere, remains little examined. The present author automatically calculated 2D inhomogeneous sections that characterize the upper mantle structure to a depth of 500–600 km.

COORDINATE CONVERSION

We can prove that travel-time curves assigned along semicircle line can be transformed, in the case of a random velocity change within the semicircle, into travel-time curves for the case of a half-plane. Assume that the velocity inside a semicircle randomly depends on two coordinates r and φ, where r coincides with the Earth's radius and the angle φ is counted clockwise, as shown in Fig. 1a.

The eikonal equation in polar coordinate system is as follows:

$$\left(\frac{\partial t}{\partial r}\right)^2 + \frac{1}{r^2}\left(\frac{\partial t}{\partial \varphi}\right)^2 = \frac{1}{v^2(r, \varphi)}, \quad (1)$$

writing the initial conditions as $t(R, \varphi_0) = 0$, $0 \le \varphi \le \pi$, where R is the Earth's radius.

Let us perform the following transformations of equation (1):

$$r^2\left(\frac{\partial t}{\partial r}\right)^2 + \left(\frac{\partial t}{\partial \varphi}\right)^2 = \frac{1}{v^2(r, \varphi)/r^2},$$

$$\left(\frac{\partial t}{\partial \ln r}\right)^2 + \left(\frac{\partial t}{\partial \varphi}\right)^2 = \frac{1}{v^2(r, \varphi)/r^2}.$$

Since we introduced division of the velocity by the radius, we shall accept the $r > 0$ limitation, i.e., the radius value is always over 0. In other words, the introduced transformations cannot be applied in the Earth's center.

Then we shall transform the variables

$$z = \ln r, \quad x = \varphi, \tag{2}$$

and obtain after the transformation

$$\left(\frac{\partial t}{\partial z}\right)^2 + \left(\frac{\partial t}{\partial x}\right)^2 = \frac{1}{\nu^2(e^z, x)/e^{2z}}.$$

Then, we designate

$$\nu(e^z, x)/e^z = w(x, z),$$

where $w(x, z)$ is a function of Cartesian coordinates. These transformations transform the time field for the semi-circle case with arbitrary two-dimensional velocity distribution in the case of a half-plane, i.e., at the planar surface of observations. The coordinate origin $r = 0$ is eliminated from consideration. The entry conditions are transformed to the form $t(\ln R, x_0) = 0$.

We shall now transfer the origin of the Cartesian coordinate system onto the $z = \ln R$ surface and change the axis z orientation to the opposite:

$$h = \ln R - z = \ln(R/r),$$

then we obtain

$$\left(\frac{\partial t}{\partial(\ln R - h)}\right)^2 + \left(\frac{\partial t}{\partial x}\right)^2 = \frac{1}{w^2(x, \ln R - h)},$$
$$\left(\frac{\partial t}{\partial h}\right)^2 + \left(\frac{\partial t}{\partial x}\right)^2 = \frac{1}{f^2(x, h)}. \tag{3}$$

Here, we designated function $w(x, \ln R - h)$ as $f(x, h)$. The entry conditions are transformed to the form $t(0, x_0) = 0$. After these transformations, the time fields correspond to Cartesian coordinates, i.e., to the planar Earth when the wave sources are located on the surface (Fig. 1b). Note, that at these transformations, the horizontal distance r is replaced with an angular offset φ (which is often designated as Δ). Seismic rays are characteristics of the eiconal equation, which are also transformed to the case of a planar half-space. Hence, the travel time curves recorded at super-long distances from the sources can be interpreted after transformations by any method that is valid for the case of planar 2D heterogeneous medium; the result after that can be transformed back to the spherical 2D heterogeneous model.

The formulas for backward inversions are as follows:

$$z = R - h,$$
$$r = e^{(r-h)} = e^r/e^h,$$
$$\varphi = \pi/2 - x, \tag{4}$$
$$\nu = fr.$$

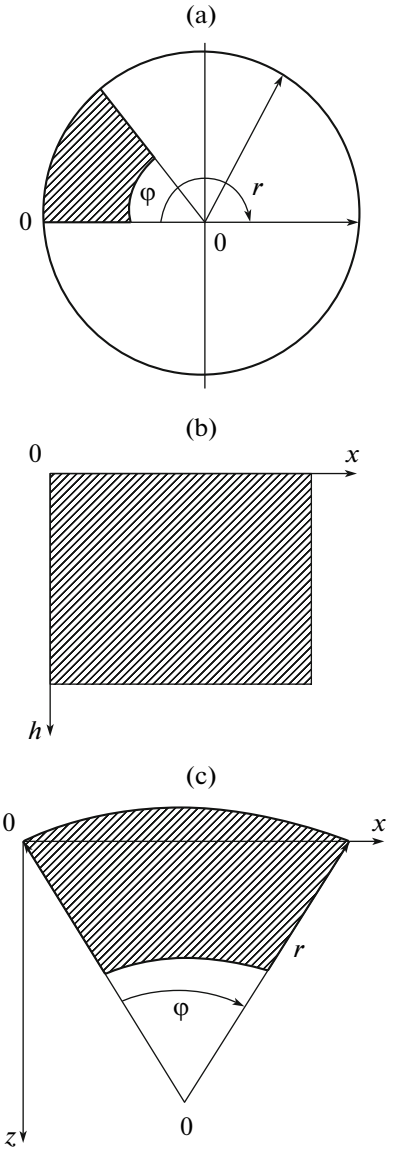

Fig. 1. Successive display of velocity fields (a–c) in the process of transformations (2)–(4).

The final section is presented in Cartesian coordinates as shown in Fig. 1c. Similar transformation formulas for transition from the spherical Earth to the planar model and backward were presented in publications [Gerver and Markushevich, 1968; Muller, 1971]; these were deduced based on an assumption of spherically symmetric Earth.

THE METHOD OF HOMOGENOUS FUNCTIONS

We applied the method of homogeneous functions [Piip, 1991, 2001] for transformations of travel-time curves obtained on superlong profiles; this is a method

of local approximation of velocity section by homogeneous functions of two coordinates. The method is widely applied for interpreting data of deep seismic sounding and engineering seismic explorations [Piip and Efimova, 1996].

The selection of an approximating function is determined by the following facts. Homogeneous functions have several properties that determine geological media. The lines of function levels are similar curves, as most interfaces are in geological sections (for instance, folded or flat-parallel media). The shape of the velocity contours of two-coordinate homogeneous functions may be random. Homogeneous functions are very suitable for the approximation of real geological sections and this has been proven in numerous publications. For example, this was proven by calculation of model computing and by comparing the reconstructed sections with borehole data. The applicability of these functions was also proven by the fact that calculated sections correspond to the details of those determined by the method of the common depth point (CDP) from a reflected-wave geophysical survey [Naumov, 2004; Piip et al., 2007]. We present below a numerical example of reconstructing the velocity section in a spherically symmetric Earth by the homogeneous function method.

Homogeneous functions are the most common two-coordinate functions applied in contemporary seismic exploration for calculating seismic velocity values by methods of simple inversion. Layered homogeneous media with flat interfaces and vertically inhomogeneous media with a random depth function are special cases of a homogeneous two-coordinate velocity function. Homogeneous two-coordinate functions do not have limitations with respect to either vertical or horizontal component of the velocity gradient and may contain rectilinear inclined lines of a velocity discontinuity, i.e., boundary surfaces. The inverse kinematic seismic problem is solved steadily and unequivocally with set of homogeneous functions continuously growing with depth [Piip, 1984]. During section approximation by continuous functions, transition zones replace the lines of velocity discontinuity.

The method of homogeneous functions is a generalization of classical methods for solving inverse kinematic problems in seismic exploration for the case of 2D inhomogeneous media. The classical methods for solving inverse problems include the plus-minus method of refracted waves and methods of calculating the effective velocity from travel time curves of reflected waves (constant difference, quadratic coordinates, etc.). The Gerglotz–Wichert–Chibisov inversion method is well known for continuous presentation of a one-dimensional medium. The method of homogeneous functions is applicable both in discontinuous media [Piip and Efimova, 1981] (containing the first type of boundaries) and in continuous media models. It was demonstrated within the homogeneous function method that the Gerglotz–Wichert–Chibisov formula is applicable in media with a large horizontal velocity gradient, namely, in the case of a first-degree homogeneous function [Piip, 1982, 1984].

The GODORGAF software package for processing travel time curves, for interpretation, and for construction of seismic sections from refracted wave data performs a local approximation of a real velocity section by continuous homogeneous functions of arbitrary degree monotonously growing with increasing polar angle. Homogeneous functions are presented in polar coordinates as

$$v = r^m \psi(\varphi), \quad (5)$$

where m is an arbitrary real number and $\psi(\varphi)$ is an arbitrary continuously growing function of the polar angle. The theory was presented in detail in [Piip, 2001]. The algorithm consists of the following. Approximation of a real section is calculated with homogeneous function (5) for each pair of reverse travel-time curves tied in reciprocal points. An important specific feature of homogenous velocity functions is that inverse 2D problems can be reduced in this case to a 1D problem using simple transforms of initial travel-time curves. In this case, opposite transformed travel-time curves are best superposed by the minimization methods and, hence, travel-time curve segments belonging to the same layer become superposed. Thus, the difficult and ambiguous problem of identifying waves on travel-time curves from different excitation points is solved automatically in the process of solving the inverse problem. The unknown function of the polar angle is calculated by using numerical methods as a growing step-wise function.

If a complex system of observed travel-time curves is interpreted, then the approximation of a real section using function (5) is independently calculated for each pair of opposite travel-time curves selected from a system of observed travel-time curves in a region where the rays, which are also calculated, penetrate; thus, a multitude of functions (5) is determined and their number is always equal to that of the pairs of opposite travel-time curves.

The general section is calculated by aggregation in the section of lower portions of local velocity fields, which are not overlain by local velocity fields corresponding to shorter pairs of opposite travel-time curves. Since inversion of seismic travel-time curves is stable with this method, then boundaries between local velocity fields are not seen in the section and they do not prevent continuous tracing of interfaces in the general section.

When all functions (5) and section regions are known where the functions approximate the section, the general section is calculated in nodes of the assigned rectangular grid, i.e., the grid section. The grid parameters cannot be selected arbitrarily, since

boundaries of local velocity fields are seen at a very small step of the grid, while discontinuities and other specific features of the field are not traceable at very large steps of the grid. Thus, the grid spacing determines the section resolution.

Linear interpolation of travel-time curves with respect to excitation points is applied for inversion of travel-time curves in cases of sparse observation systems. N.N. Puzyrev suggested the interpolation formulas applied by the present author in 1963. A section of equal offsets is constructed as an intermediate stage of the interpolation. This is a time section where the specific features of a real deep section are reflected, as is shown in [Piip, 2001].

The automatically calculated deep sections are a velocity field assigned in nodes of a rectangular grid. This velocity field contains information on interfaces and tectonic dislocations. We present the velocity field as a surface with shaded relief for visualizing discontinuities and faults in the sections. Computers provide to ability to visualize surfaces. With lighting from above, first-type boundaries (where velocity increases at the discontinuity step-wise downward) look like light-colored lines. Inversion boundaries (where the velocity decreases step-wise downward) look like dark lines. Second-type discontinuities, where the velocity gradient changes step-wise, look like boundaries between layers of different light intensity. The image of a velocity field as a surface with lighted relief is combined with a field of velocity contours. This provides knowledge of velocity changes in section layers.

We repeatedly calculated theoretical travel-time curves in sections recorded by the method of homogeneous functions and they always coincided with the observed curves sufficiently well. The root-mean-square deviations lie within the admissible values accepted during the evaluation of sections in present-day interpretation.

A *Numerical example* is used for illustrating the performed transformation and determining the limits of applicability; we inverted the Jeffreys–Bullen travel-time curve using the method of homogeneous functions.

The table time values in Jeffreys–Bullen travel-time curve were presented in [Jeffreys, 1980]. Only a 1D growing-velocity dependence upon the Earth's radius can be calculated from a single travel-time curve. The 1D velocity function is a specific case of a homogeneous two-coordinate function. It is calculated automatically if the direct and reverse travel-time curves are identical. The initial observation system for recovery of a spherically symmetrical Earth was assigned as the reflection of two reverse Jeffreys–Bullen travel-time curves mirror symmetrical to one another with an angular distance between the sources of 180°.

The inversion algorithm is such that, if two opposite travel-time curves are given, then only a growing homogeneous velocity function can be calculated. For obtaining a nonmonotonic velocity dependence, including waveguides, a complete observation system is needed where sources and receivers are arranged in equal steps. For inversion we used travel-time curves identical to the Jeffreys–Bullen travel-time curve with sources located at each observation point, i.e., at an angular distance between sources of 5° (Fig. 2a). These travel-time curves taken together made 640 pairs of opposite travel-time curves. These travel-time curves were displayed depending on the angular coordinate, i.e., transformations (2) were already performed for them, and therefore inversion of these travel-time curves by the method of homogeneous functions reduces them to a planar Earth. The velocity function (5), i.e., the local velocity field, was calculated independently for each pair of opposite travel-time curves during processing. The final plane-parallel section constructed by aggregation of all 640 local velocity fields is shown in Fig. 2b. The boundaries of local fields are not seen in this figure, since the inversion algorithm is stable and unambiguous. The depth of the calculated section is 0.9, which corresponds to an r/R ratio of 0.9. At greater depth, the section becomes mutilated since, according to formulas (1–4), limitations to the depth of the section exist. We obtained a limitation for performing transformations $R - r =$ 3770 km. Then, the plane-parallel section was transformed into a section for semi-circle using formula (4). The known discontinuities in the Earth section are distinctly discernible in the section (Fig. 2), viz., the boundaries of the crust, upper and lower mantle, and outer core. The section was calculated to a radial depth of 3770 km.

The velocity calculation error can be evaluated by comparing the known1D velocity function for a spherically symmetrical Earth with that calculated using homogeneous functions (Fig. 2d). The velocity dependence was sufficiently accurately calculated to the outer core boundary. The velocity within the outer core turned out approximately 35% higher. This is explained by the fact that velocity within a waveguide cannot be accurately calculated only from the first P-waves.

DATA INTERPRETATION AND ITS RESULTS

We present here the results of 2D interpretation of travel-time curves along five superlong profiles, viz., Quartz, Craton, Kimberlite, Meteorite, and Rift. The profile layout is shown in Fig. 3a. The recognized structural features are displayed in all profiles and therefore we shall discuss them jointly. The most complete observation system was recorded along the Craton profile. Travel-time curves from four sources were traced along the whole profile over a distance of 3500 km. Long travel-time curves from three sources were recorded almost along the whole length of the Kimberlite profile over a distance of 2700 km.

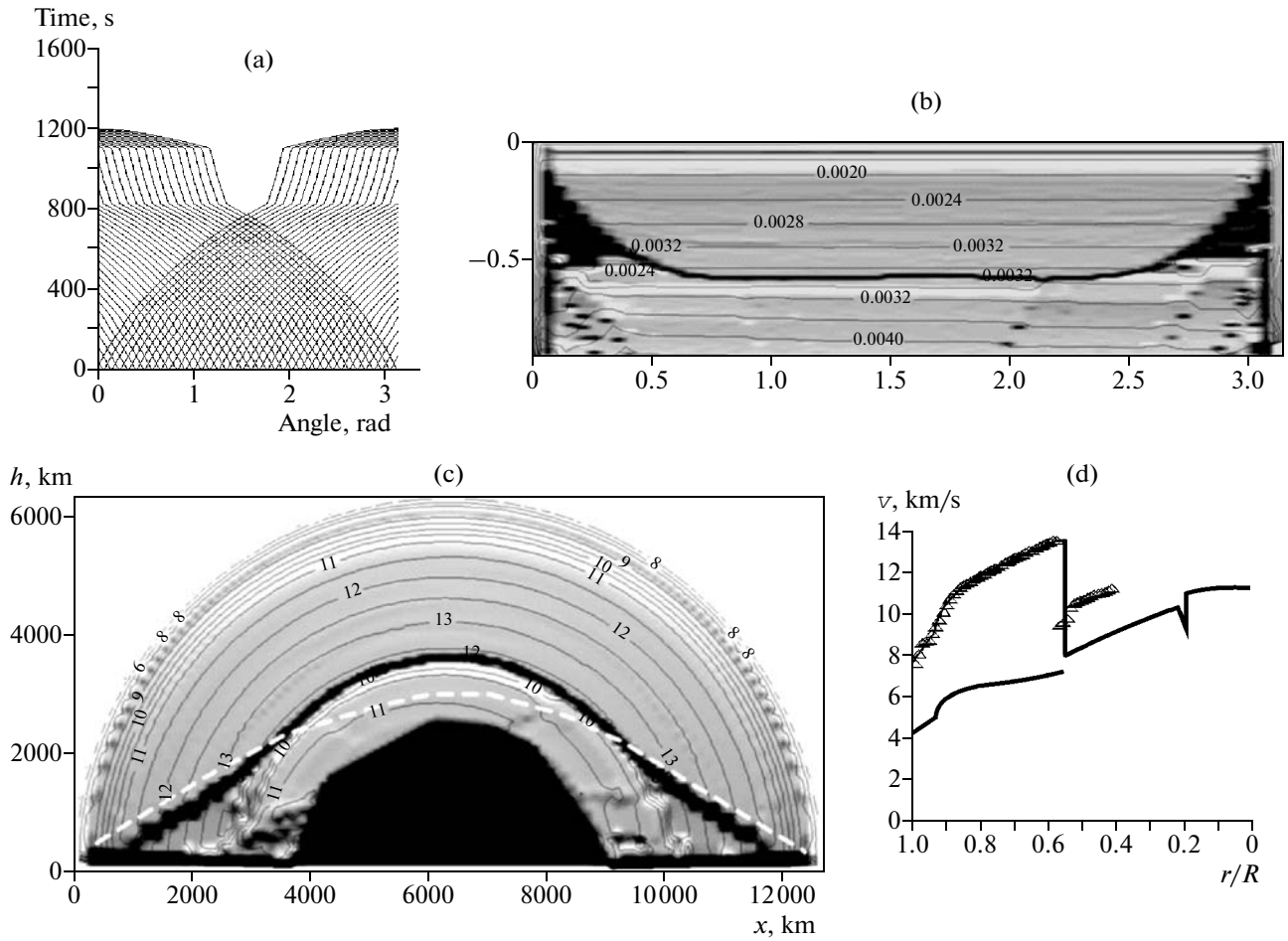

Fig. 2. Calculation of the Earth section by the method of homogeneous functions: (a) Jeffreys–Bullen travel-time curves; (b) intermediate section for flat surface (contours correspond to v/r values there, v is velocity and r is distance to the Earth's center); (c) section of round Earth, the dashed line limits the region of correct recovery of the section; (d) comparison of the known dependence of velocity upon the radius (solid line) and calculated dependence using the method of homogeneous functions (triangles).

The records of the first arrivals of waves along the Quartz superlong profile, which extends from the Altai–Sayan fold zone in the southeast to the Pechora syneclise in the northwest traversing the West Siberian plate and the Urals, were obtained from three sources. The travel-time curve is over 3900 km long; the travel-time curves are shown in Fig. 3b. However, the branches of travel-time curves from sources 1150 and 2050 km (the northern and southern branches, respectively) do not have opposite travel-time curves, and therefore we can calculate only 1D velocity dependences here. The observation system was supplemented by two synthetic travel-time curves from sources of 250 and 3000 km with the purpose of using these branches for constructing homogeneous functions. The starting portions of both travel-time curves were accepted as being identical to opposite travel-time curves from neighboring sources and the remote branches were recovered using time records in reciprocal points shown by circles in Fig. 3b. I shall note that these travel-time curves were used for constructing the section in a pair with an observed opposite travel-time curve.

The time sections of equal offsets were constructed at all profiles for interpolating the travel-time curves and for controlling the automatically calculated sections with the purpose of confirming that the structural features obtained in the sections really exist in the observed time field. Figure 3c presents a time section of equal offsets in the Quartz profile constructed at a reduction of 20 km/s. The distance of equal offset lines is in inverse proportion to the apparent velocity. We can discern in the time section first-type boundaries (or narrow transition layers) as extensive zones of contour closeness and inversion interfaces as upper boundaries of regions of lowered apparent velocity. One can distinguish in the time section, as shown in Fig. 3c, the Earth's crust, high-velocity layers in the lithosphere, and three local regions of lowered velocity at reduced time intervals of approximately 70 seconds. These regions are regularly distributed and are of approximately equal dimensions. We shall show below

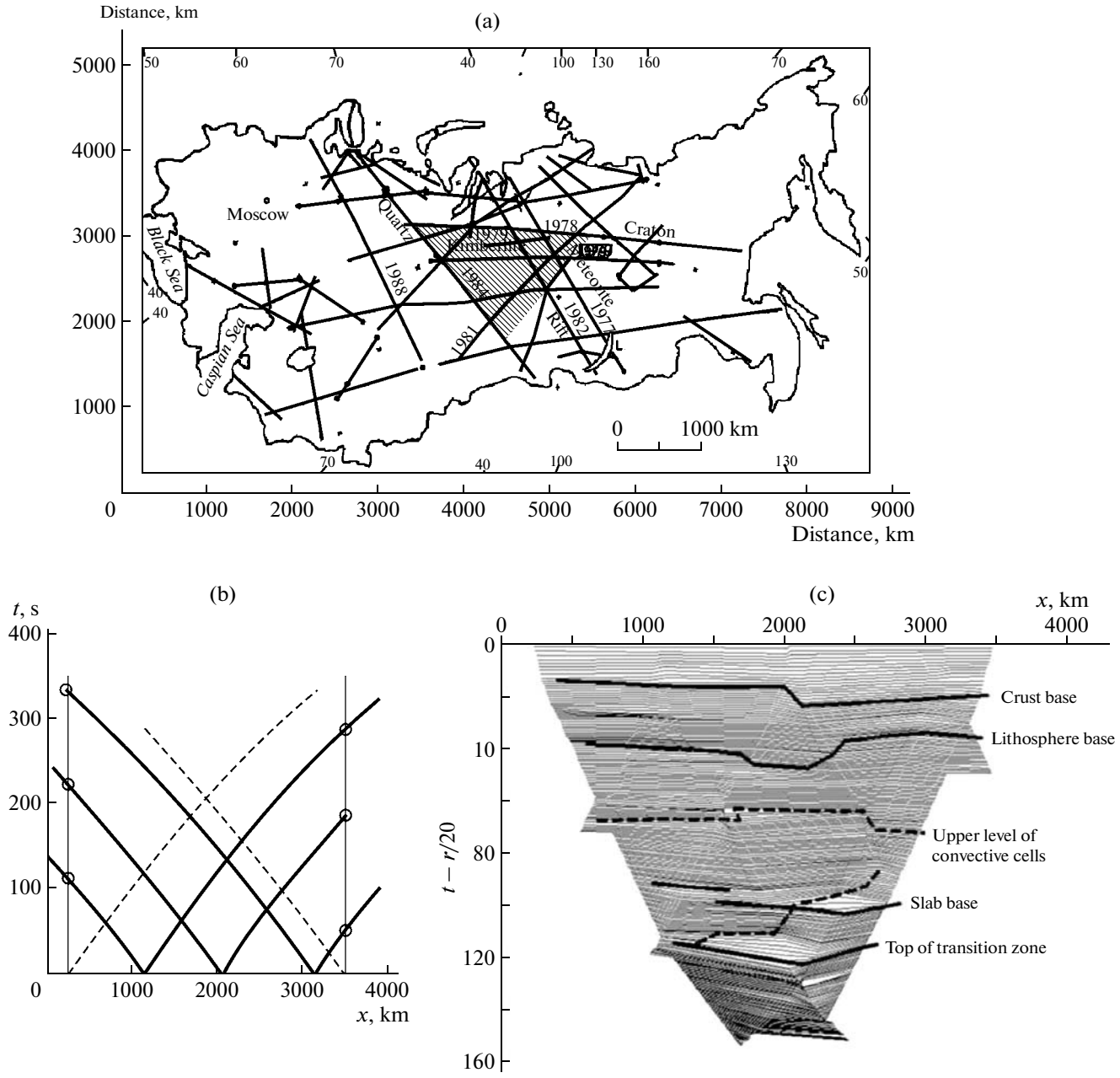

Fig. 3. (a) Layout of examined profiles (the region where the spherical velocity slice of the upper mantle was recorded is hatched); (b) travel-time curves of first waves along the Quartz profile (circles are reciprocal times used for recovery of travel-time curves from sources 250 and 3500); (c) section of equal offsets along the Quartz profile (contour interval is 10 km, specific features corresponding to main interfaces in the Earth are shown in the section).

that these local regions were interpreted as convective cells. The upper boundary of the transition zone between the low and upper mantle, which is very complex and heterogeneous, is clearly visible.

When constructing the sections, we applied interpolation of observed travel-time curves with a source interval of 90 km and receiver interval of 15 km. The interpolated travel-time curves were used for inversion.

The sections along five superlong profiles in Siberia were constructed with allowance for the Earth's curvature (Figs. 4a–4c). The independently calculated sections correlate well with each other. Seismic rays in the Craton, Kimberlite, and Quartz profiles reached a depth of 500–600 km, where the transition zone between the upper and lower mantle is traceable. The section depth along the Rift and Meteorite profiles did not exceed 250 km. The velocity field was calculated in all profiles in the nodes of a rectangular grid measuring 30×10 km. The cell dimensions determine the resolution of the section and, therefore, we cannot deter-

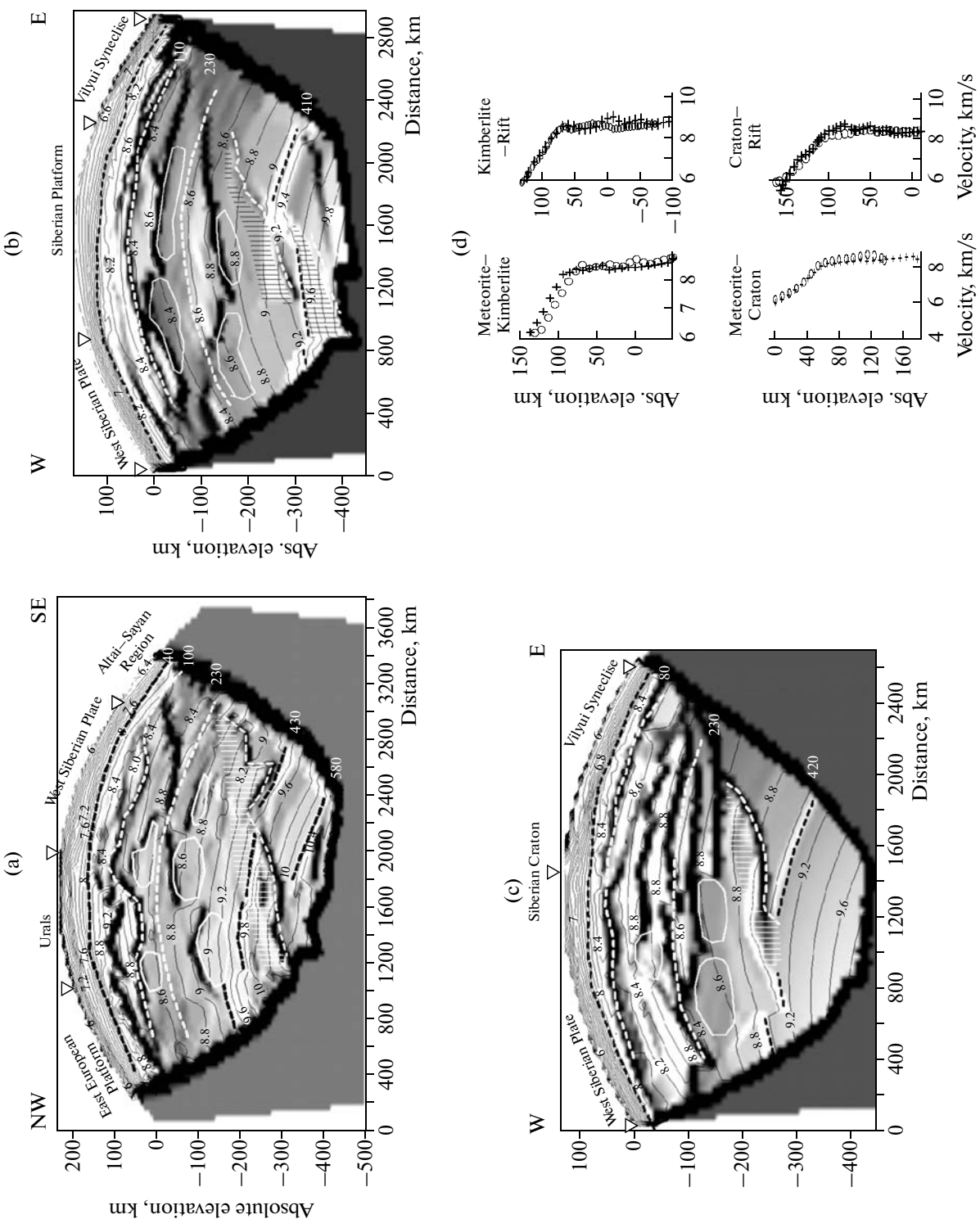

Fig. 4. Seismic sections along the Quartz (a), Craton (b), and Kimberlite (c) profiles and their structural interpretation. Dashed lines show interface boundaries. Convective cells are outlined with solid lines. Subducted slab is hatched. Thin lines are velocity contours with an interval of 0.2 km/s. White numerals to the right show interface depths, triangles show location of nuclear explosions; comparison between vertical velocity dependences at the sites of profile intersections (d), crosses are velocity values in E–W-trending profiles, circles are same in N–S-trending profiles.

mine whether the interfaces are sharp, step-wise changes in the velocity, or narrow transitional velocity zones up to 10–15 km thick. The following layers were distinguished in all automatically calculated sections without using any a priori data: the Earth's crust, lithosphere, asthenosphere, and a transition layer between the upper and lower mantle.

The *Crust* was observed in sections as a layer of higher velocity gradient. The crust is 50 km thick under the Siberian platform. The crust thickness is approximately 40 km thick under the West Siberian plate and Vilyui syneclise. It decreases to 35 km in the Altai–Sayan fold belt and it increases to 75 km in the Ural mountainous region. Then, the crust thickness decreases to 40–45 km under the East European platform. The crust base is traceable continuously in all sections as a second-type interface with a jump in the velocity gradient.

The seismic velocity in the subcrustal *lithosphere* changes from approximately 7.8 to 8.8 km/s. In the examined profiles the subcrustal lithosphere has a one- or two-layer structure and a lower velocity gradient relative to the crust. A two-layered subcrustal lithosphere of a higher thickness (up to 130 km) and velocity (up to 9 km/s) was recorded along the Quartz profile in the Ural mountainous region. The thin one-layer subcrustal lithosphere is 35 km thick in the Altai–Sayan fold zone and the velocity in it changes from 8 to 8.2 km/s. A very thin (20 km) subcrustal lithosphere (the velocity is from 8 to 8.4 km/s) was recorded along Kimberlite profile. The lithosphere in the southern portion of the N–S-trending Rift profile showed the same structure. The lithosphere thickness increases to 80 km in the northern portion of this profile and its structure becomes more complex. The lithosphere thickness is 110 km along Craton profile, as an average, and the velocity grows at its base to 8.5 km/s. The base of the lithosphere is an inversion (the velocity above the interface is higher than at the top of the underlying layer) curvilinear discontinuity with a variable velocity above and below the interface.

The *Asthenosphere* shows velocity values, ranging from 8.4 to 8.7 km/s, and lowered velocity gradient. A Lemann discontinuity underlies the asthenosphere. It is an almost flat, i.e., practically spherical, very weak (velocity contrast) interface of alternating sign. It is traceable at a constant depth of 220–230 km. The Lemann discontinuity is recognized from the following indicator: not a single structural feature of the asthenosphere or subasthenospheric upper mantle crosses it.

The same position of the asthenosphere base was determined from investigating the upper mantle structure by surface waves along the MOBAL-2003 profile [Rasskazov et al., 2007] crossing the central part of the Siberian platform up to Gobi Altai. The authors of this publication found that the base of the low-velocity layer at the level of 190–210 km corresponds to the Le Mann cratonic discontinuity.

From our data, the asthenosphere is characterized by a complex structure strongly variable along profiles. Round regions with velocity lowered to 8.4 km/s were recorded on Craton and Quartz profiles within the asthenosphere.

The asthenosphere and the upper mantle underlying it have different structure. Round elongated regions with a lowered velocity (8.2–8.6 km/s) and velocity gradient were recorded in the *subasthenospheric upper mantle* with velocities ranging from 8.6 to 9.2 km/s. These regions can be interpreted as convective cells. The cell dimension in the upper mantle, measured on a roughly vertical plane, is 500 × 100 km, as an average. It is possible that two-stage convection exists in the examined profiles if we consider the local regions of lower velocity in the asthenosphere and subasthenospheric mantle as convective cells. The two convective stages are separated by the Le Mann discontinuity. Local low-velocity anomalies of similar dimensions (700 × 160 km) were also recognized in a 3D tomographic model of the upper mantle in Asia [Yanovskaya and Kozhevnikov, 2003]; they were interpreted as plumes.

The top of the transition zone between the upper and lower mantle is traceable at a depth ranging from 350 to 450 km as a sharp first-kind interface (or a narrow transition zone) with a velocity jump from 9–9.2 km/s to 9.4–9.6 km/s. The top of the transition layer has very complex relief on all deep profiles. Reeberg and his colleagues [Reeberg et al., 1997] examined the relief on top of the transition zone in long refracted-wave profiles, and they noted its complex relief. A sharp depression up to 50 km deep was noted in the central part on top of the transition zone in all three deep profiles, where a high-velocity slab is descending. The slab is immersed from the side of the Vilyui syneclise (Craton and Kimberlite profiles) or from the side of the Altai–Sayan fold region (Quartz profile). The slab thickness is approximately 50–100 km. A slab is an extensive inclined elongated zone of higher seismic velocity. The lower boundary of the slab is distinctly discernible in all profiles as a continuous inversion boundary, while the upper boundary is less distinctly discernible. The slab breaks through the top of the transition zone in all deep profiles, while it breaks through the whole of the transition zone to the lower margin of the section in Quartz profile.

A sharp first-type boundary with a velocity jump from 10.2 to 10.4 km/s was recorded in Quartz profile at a depth of 580 km.

EVIDENCE OF THE RELIABILITY OF THE SECTIONS

1. All principal interfaces in the lithosphere and upper mantle were obtained in all automatically calcu-

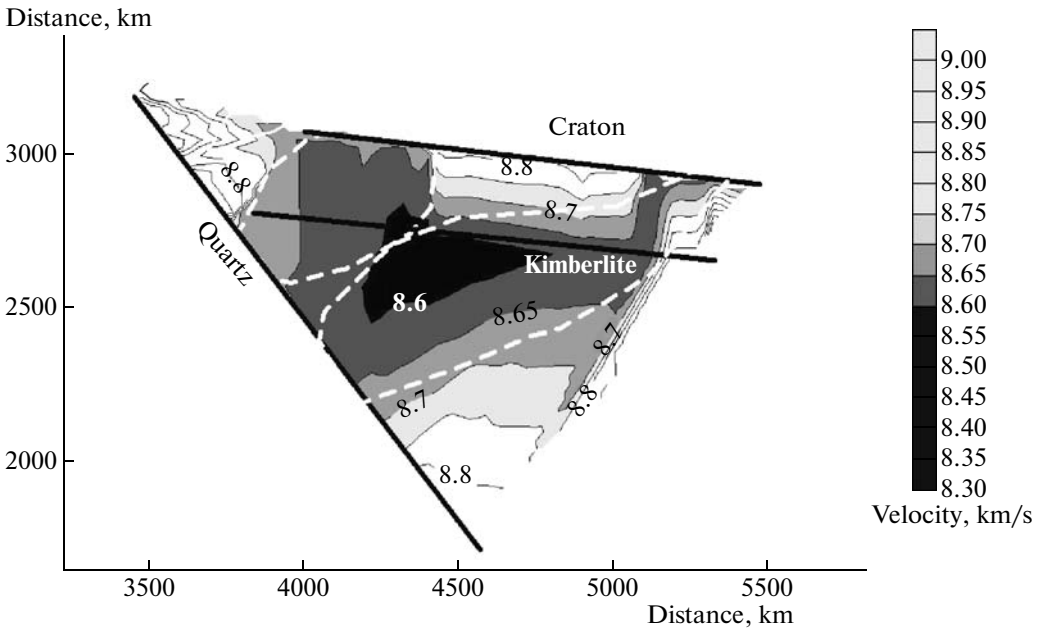

Fig. 5. Spherical velocity slice at a depth of 290 km. White dashed line shows contours of convective cells, thin lines are velocity contours, velocity scale is shown on the left.

lated sections without using any a priori information. A high-frequency slab (with velocity elevated by 0.2 km/s) and several round regions (convective cells) with velocities lowered by 0.2 km/s were recorded in the upper mantle in all deep sections.

2. The structural features obtained in the profiles are visually discernible in the observed time fields (sections of equal offsets).

3. The independently calculated sections are well coineided with each other at the intersection points of profiles (Fig. 4d). In this case, not only do the velocity values coincide well at the intersections points (with a root-mean-square error of 0.08 km/s) but the structural feature boundaries coincide there, too.

3D images of structural features in the upper mantle. We constructed a velocity spherical slice at a radial depth of 290 km for the purpose of accessing the arrangement of cells in plan view (Fig. 5). This depth approximately corresponds to the upper limit of cell location in the subasthenosperic mantle. For delineating the cell boundaries in the slice (white dashed line), we visually used sections along profiles, since the profile network is very loose. We recognized a northeastern trend of the convective cells. The cell dimensions are $1000 \times 500 \times 100$ km. The coordinates of the spherical velocity slice coincide with the coordinates on the map of the profile layout (Fig. 3a).

GEOLOGIC–TECTONIC INTERPRETATION OF THE SECTIONS

The following geodynamic interpretation of events suggested by A.M. Nikishin [Nikishin, 2002] and explaining the trap origin in West Siberia is accepted as the most suitable: "under West Siberia, subducted lithospheric slabs were separated from overlying lithosphere and a general descending mantle flow existed. The plume material rose behind the regions of descending flows, which, possibly, stimulated the plume ascent." There is an opinion that ascending plumes give rise to mantle convection in the upper mantle [Lobkovskii et al., 2004].

CONCLUSIONS

1. The crust base displayed itself in sections as a sharp type-two boundary with a negative jump of its velocity gradient.

2. The subcrustal lithosphere shows a complex structure and variable thickness that strongly varies depending upon the structural elements of the crust.

3. The asthenosphere is underlain by the Le Mann spherical discontinuity lying at a depth of 220–230 km.

4. Local round inhomogeneities of lower velocities were revealed in sections in the upper mantle, which can be interpreted as convective cells and a subducted slab, i.e., an inclined layer of higher velocity transecting and breaking through the transition zone surface.

5. The surface of the transition zone between the upper and lower mantle displayed itself in all deep sections as a sharp type-one boundary with a velocity jump from 9–9.2 to 9.4–9.6 km/s, with complex relief, and a depth varying from 350 to 450 km.

6. A sharp type-one boundary was recorded at a depth of 580 km within the transition zone in section along the Quartz profile.

REFERENCES

Egorkin, A.V., Zyuganov, S.K., and Chernyshev, N.M., Upper Mantle of Siberia, in *27-i Mezhdunar. geol. kongress. Geofizika. Sektsiya 8* (27th Intern. Geol. Congr. Geophysics. Section 8), Moscow: Nauka, 1984.

Gerver, M.L. and Markushevich, V.M., Properties of Traveltime Curve from a Surface Source, in *Nekotorye pryamye i obratnye zadachi seismologii. Vychislitel'naya seismologiya. Vyp. 4* (Some Direct and Inverse Seismologic Problems. Computational Seismology, Issue 4), Moscow: Nauka, 1968.

Jeffryes, H., *Zemlya, ee proiskhozhdenie, istoriya i stroenie* (The Earth: Its Origin, Evolution, and Structure), Moscow: Inostr. lit, 1980.

Lobkovskii, L.I., Nikishin A. M. and) Khain V.E. *Sovremennye problemy geotektoniki i geodinamiki* (Contemporary Problems in Geotectonics and Geodynamics), Moscow: Nauchnyi mir, 2004.

Mechie, J., Egorkin, A.V., Fush, R., et al., P-Wave Mantle Velocity Structure Beneath Northern Eurasia from Long-Range Recordings Along the Profile Quartz, *Phys. Earth Planet. Inter.,* 1993, vol. 79, pp. 269–286.

Muller, G., Approximate Treatment of Elastic Body Waves in Media with Spherical Symmetry, *Geophys. J. Roy. Astron. Soc.*, 1971, vol. 23, no. 4, pp. 435–449.

Naumov, A.N., Effektivnost' interpretatsii dannykh inzhenernoi seismorazvedki metodom odnorodnykh funktsii, *Vestn. Mosk. Univ. Ser. 4.Geologiya*,

Nikishin, A.M., Tectonic Settings, in *Vnutriplitnye i okrainno-plitnye protsessy* (Intraplate and Marginal Plate Processes), Moscow: Mosk. Gos. Univ. Ser., Geologiya, 2002.

Pavlenkova, G.A. and Solodilov, L.N., Fragmented Structure of Upper Layers of the Mantle, *Fiz. Zemli*, 1997, no. 3, pp. 11–20.

Pavlenkova, N.I., Pavlenkova, G.A., and Solodilov, L.N., High Velocities in the Uppermost Mantle of the Siberian Craton, *Tectonophysics*, 1996, vol. 262, pp. 51–65.

Piip, V.B. and Efimova, E.A., Construction of Refracting Interfaces in Variable-Velocity Media, in *Prikladnaya geofizika* (Applied Geophysics), Moscow: Nedra, 1981, issue 90, pp. 31–46.

Piip, V.B., 2D Inversion of Refraction Traveltime Curves Using Homogeneous Functions, *Geophysical prosp.*, 2001, vol. 49, pp. 461–482.

Piip, V.B., Local Reconstruction of a Seismic Section from Refracted Wave Data Based on Homogeneous Functions, *Fiz. Zemli*, 1991, no. 10, pp. 24–32.

Piip, V.B., New Methods of Interpreting Time Fields in Variable-Velocity Media, *Vestn. Mosk. Univ. Ser. 4, Geologiya*, 1984, no. 3, pp. 83–92.

Piip, V.B., A Simplified Method of Constructing Velocity Contour Sections from Traveltime Curves of First Arrivals, in *Applied Geophysics*, Moscow: Nedra, 1982, issue 105, pp. 82–88.

Piip, V.B., Zhamozhnyaya, N.G., and Suleimanov, A.K., Detailed Velocity Structure of Salt Domes in the North Caspian Basin from Refraction Data, *First Break*, 2007, vol.25, pp. 99–103.

Piip, V.B. and Efimova, E.A., Investigation of Deep Structure of the East- European Platform Using Seismic Refraction Data, *Oil and Gas in Alpidic Thrust Belts and Basins of Central and Eastern Europe. EAGE Spec. Publ.*, 1996, vol. 5, pp. 283–288.

Rasskazov, S.V., Chuvashova, I.S., Mordvinova, V.V., and Kozhevnikov, V.M., The Role of Lemann Cratonic Interface in the Cenozoic Dynamics of the Upper Mantle in Central Asia: Interpretation of Models of Seismic Wave Velocities in the Light of Spatiotemporal Evolution of Volcanism, in *Fundamental'nye problemy tektoniki. Materialy 40-go Tektonicheskogo soveshchaniya. T. 2* (Fundamental Problemsin Tectonics. Proceedings of 40th Tectonic Conference, vol. 2), Moscow: GEOS, 2007.

Reeberg, T., Mechie, J., Ventzel, F., et al., Specific Features of Transition Zone in Mantle of North Eurasia, in *Struktura verkhnei mantii Zemli* (Structure of the Earth's Upper Mantle), Moscow: GEOS, 1997.

Vinnik, L.P. and Egorkin, A.V., Wave Fields and Models of the Lithosphere from Data of Seismic Studies in Siberia, *Dokl. Akad. Nauk SSSR*, 1980, vol. 250, no. 2, pp. 318–320.

Yanovskaya, T.B. and Kozhevnikov, V.M., 3D S-Wave Velocity Pattern in the Upper Mantle Beneath the Continent of Asia from Raleigh Wave Data, *Phys. Earth Planet. Inter.*, 2003, vol. 138, pp. 263–278.